

Study of Substituent Effects on the Photoconductivity of Soluble 2,(3)- and 1,(4)-Substituted Phthalocyaninato- and Naphthalocyaninatotitanium(IV) Oxides

Götz Winter,[†] Heino Heckmann,[†] Peter Haisch,[†] Wolfgang Eberhardt,[†] Michael Hanack,^{*,†} Larry Lüer,[‡] Hans-Joachim Egelhaaf,[‡] and Dieter Oelkrug^{*,‡}

Contribution from the Institut für Organische Chemie, Lehrstuhl für Organische Chemie II, Auf der Morgenstelle 18, and Institut für Physikalische Chemie, Auf der Morgenstelle 8, Universität Tübingen, D-72076 Tübingen, Germany

Received May 11, 1998

Abstract: Soluble alkyl (**II**, **8a,b**), fluoroalkyl (**4a**), and fluoroalkoxy (**4b,c**, **8c**) 1,(4)- or 2,(3)-substituted phthalocyaninato- and linear 2,(3)- and angular 1,(2)-annulated naphthalocyaninatotitanium(IV) oxides **10**, **12**, and **14** were synthesized and characterized with regard to their spectroscopic, photophysical, and photochemical properties. While alkyl- and fluoroalkoxy-substituted compounds are highly soluble in nonpolar solvents, e.g., hexane, fluoroalkyl-substituted compounds are better soluble in polar aprotic solvents such as acetone. The stability against photooxidation in solution is enhanced on going from alkylated phthalocyanines 1,(4)-(C₅H₁₁)₈PcTiO (**8a**), 1,(4)-(C₆H₁₃)₈PcTiO (**8b**), and 2,(3)-(C₄H₉)₈PcTiO (**II**) to fluorinated phthalocyanines 2,(3)-(CF₃)₄PcTiO (**4a**), 2,(3)-(CF₃CH₂O)₄PcTiO (**4b**), and 2,(3)-(CF₃CH₂O)₈PcTiO (**4c**), from phthalocyanines to naphthalocyanines (*tert*-butyl)₄-2,(3)-NcTiO (**10**), 1,(2)-NcTiO (**12**), and (*tert*-butyl)₄-1,(2)-NcTiO (**14**), and on going from 2,(3)-substituted **4a–c** to 1,(4)-substituted phthalocyanines **8a–c**. Thin films of these compounds, prepared by either vacuum deposition or spin casting, are classified into three types according to increasing intermolecular π - π interactions. Type α films, characterized by absence of exciton splitting, are formed from 1,(4)-substituted phthalocyanines **8a–c**. These films show low dark conductivities and photoconductivities and are considerably sensitive to photooxidation. Type β films, characterized by weak exciton splitting, are formed from fluorinated phthalocyanines **4a–c** as well as from rapidly deposited 2,(3)-substituted phthalocyanines **II** and the unsubstituted PcTiO (**I**). These films show enhanced photoconductivity and are generally more stable against photooxidation than type α films. Type γ films, formed by slow deposition of **II**, **10** and unsubstituted phthalocyanine **I**, are classified by a largely red-shifted B-band absorbing in the near-IR. These films are highly photosensitive as well as stabilized against photooxidation. Steady-state photoconductivities and dark conductivities in thin films are strongly dependent on oxygen partial pressure. Alkylated PcTiO's such as **8a**, **8b**, and **II** are found to be p-type conductors (positive oxygen influence on conductivities) like unsubstituted PcTiO (**I**), whereas angularly annulated naphthalocyanines such as **12** and **14** as well as fluorinated PcTiO's **4a–c** are n-type conductors (negative oxygen influence on conductivity). These findings are rationalized by comparison with experimental and theoretical literature data.

Introduction

Phthalocyanines represent an important class of organic photoconductors extensively used in organic xerographic photo-receptors, attracting considerable attention due to their high photosensitivity in the near-infrared region (600–850 nm).¹ In particular, phthalocyaninatotitanium(IV) oxide (PcTiO (**I**), Figure 1) merits close attention, since it is known to be a very potent charge generation material (CGM).^{2a} This property and

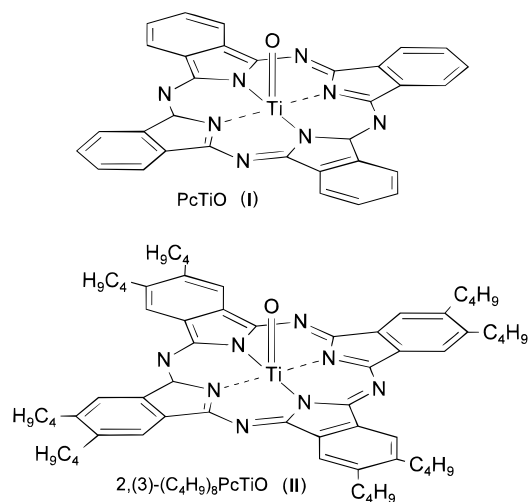


Figure 1.

the possibility of preparing flexible films² led to its use in photostatic machines or GaAsAl laser printers. Research has

[†] Institut für Organische Chemie, Eberhard-Karls Universität Tübingen.

[‡] Institut für Physikalische Chemie, Eberhard-Karls Universität Tübingen.

(1) (a) Leznoff, C. C.; Lever, A. B. P., Eds. *Phthalocyanines, Properties and Applications*; VCH: New York, 1989–1996; Vols. 1–4. (b) Hanack, M.; Lang, M. *Adv. Mater.* **1994**, *6*, 819. (c) Hanack, M.; Heckmann, H.; Polley, R. In *Methods of Organic Chemistry (Houben Weyl)*, 4th ed.; Schaumann, E., Ed.; Thieme: Stuttgart, 1997; Vol. E9d, p 717.

(2) (a) Law, K.-Y. *Chem. Rev.* **1993**, *93*, 449. (b) Yonehara H.; Pac, C. *Mater. Res. Soc. Symp. Proc.* **1994**, *328*, 301. (c) Fujimaki, Y.; Tadokoro, H.; Oda, Y.; Yoshioka, H.; Homma, T.; Moriguchi, H.; Watanabe, K.; Kinoshita, A.; Hirose, N.; Itami, A.; Ikeuchi, S. *J. Imaging Technol.* **1991**, *17*, 202. (d) Ghosez, P.; Côté, R.; Gastonguay, L. *Chem. Mater.* **1993**, *97*, 8026. (e) Arishima, K.; Hiratsuka, H.; Tate, A.; Okada, T. *Appl. Phys. Lett.* **1982**, *40*, 279. (f) Mizuguchi, J.; Rihs, G.; Karfunkel, H. R. *J. Phys. Chem.* **1995**, *99*, 16217.

shown that the photocarrier generation efficiency of **I** and related compounds depends not only on the central metal atoms but also on the crystal structure,^{2f,3,4} while different polymorphs of the same molecular materials usually have quite different photoconductive properties. **I** shows this kind of polymorphism. Unsubstituted **I** was synthesized first in 1963 by Taube,^{5a} while we published for the first time the crystal structures of two polymorphs of **I** in 1982, phase I (monoclinic; $P2_1/c$, $Z = 4$) and phase II (triclinic; $P\bar{1}$, $Z = 2$).⁶ A mixture of phases I and II is obtained by using the synthesis of **I** of Block and Meloni.^{5b} In 1987, the photoconducting properties of **I** were described,⁷ and since 1991, **I** has found use as a CGM in photostatic machines. The investigation of the photoconductivity in the various polymorphs of PcTiO has been documented in a large number of patents.⁸ There are different types of nomenclature of the polymorphs in the literature: I, II, III, IV; A, B, C, Y; or β , α , m, γ , respectively, which are used synonymously. Of particular interest is the polymorph usually referred to as Y-PcTiO (**I**), with a characteristic X-ray powder diffraction peak at 27.2,^{2a,7b,c} showing quantum efficiencies of carrier generation approaching unity at high fields.^{1,2a,3,9} Nalwa et al. achieved a phase transformation of the amorphous phase to the phases I, II, and Y by vapor treatment.¹⁰ Rietveld analyses of phase Y have been done by carrying out the refinement in a monoclinic unit cell^{9b} as well as in a triclinic cell.¹¹ Molecular modeling calculations¹² pointed to the fact that the results of the monoclinic refinement are in better agreement with the observed diffraction pattern. The molecular arrangement in phase Y is similar to that of phase I and characterized by a void between two adjacent molecules.^{9,13} Phase III (m-) PcTiO is available on acid pasting with octachloro-PcTiO and is characterized by an interplanar distance of $d = 3.8 \text{ \AA}$.¹⁴ Additionally, an

amorphous phase has been described by several authors.¹⁵ Yamashita et al. investigated the phase-selective formation of PcTiO films depending on substrate temperature and evaporation rate,^{15a} and temperature-dependent absorption spectra of different polymorphs of **I** have been published.¹³ Gulbinas et al.¹⁶ found by means of fluorescence and photocurrent measurements (exciton-exciton annihilation) that charge carriers are generated during only a short time interval, much shorter than the fluorescence-state lifetime after the exciton was created. The samples were prepared by dispersing **I** in polyvinylbutyral solution and coating onto a glass slide with transparent conductive SnO₂. The authors did not specify the type of polymorph they investigated.¹⁶ Hinch and Voll¹⁷ obtained high photosensitivity in the near-infrared and the visible spectral regions by using a mixture of charge generation pigments such as phthalocyaninatotitanium oxide and indium with different axial ligands (O²⁻, Cl⁻, OH⁻), which were prepared by coprecipitation from organic solvent/trifluoroacetic acid solution. The electrical data of these composite compounds indicate that, for example, PcInCl can be incorporated into the X-form (Y-phase) of the **I** lattice at high concentrations with minimal change in photosensitivity.¹⁷ Recently, Popovic et al.¹⁸ pointed out that the relative positions of neutral and CT excited states are a primary determinant of high carrier generation efficiency. When the CT state is close to or below the lowest lying neutral excited singlet state in the Y-phase of **I**, high carrier generation efficiencies are observed. A general methodology, based on time-resolved fluorescence quenching measurements, is proposed to determine the neutral or CT character of a state involved in charge generation.¹⁸

In our preceding studies, we described the synthesis and some photophysical as well as photochemical properties of soluble phthalocyaninatotitanium oxides [2,(3)-R₃PcTiO], with R = propyl, butyl (**II**) (Figure 1), pentyl, ethyloxy, pentyloxy (**III**), and octyloxy substituents in the periphery of the phthalocyanine ring.^{19a} Compared to unsubstituted **I**, these compounds are highly soluble in organic solvents, which allows purification by column chromatography and preparation of thin films by spin coating. The observed photooxidation of these compounds in solution can be suppressed by exclusion of oxygen.

In the present study, we compare the photoconductivities of different 2,(3)- and 1,(4)-substituted phthalocyaninato- and linear 2,(3)- and angular 1,(2)-naphthalocyaninatotitanium(IV) oxides in order to contribute new information for a better understanding of the carrier generation process. As we have already shown in our previous papers,¹⁹ substitution in the periphery of the phthalocyanine macrocycle not only affects the electronic states but also produces structural changes in the solid phase. It was observed by many authors that the photoconductivity of unsubstituted **I** increases on going from the amorphous to the crystalline phase.^{1,2a,4} Mizuguchi et al.^{2f} investigated the

(3) Saito, T.; Sisk, W.; Kobayashi, T.; Suzuki, S.; Iwayanagi, T. *J. Phys. Chem.* **1993**, *97*, 8026.

(4) (a) Popovic, Z. D.; Hor, A. M. *Mol. Cryst. Liq. Cryst.* **1993**, *228*, 75. (b) Popovic, Z. D. *Chem. Phys.* **1984**, *86*, 311. (c) Popovic, Z. D. *J. Chem. Phys.* **1982**, *76*, 2714.

(5) (a) Taube, R. Z. *Chem.* **1963**, *3*, 194. (b) Block, R.; Meloni, E. G. *Inorg. Chem.* **1965**, *4*, 111.

(6) Hiller, W.; Strähle, J.; Kobel, W.; Hanack, M. *Zeitschr. Kristallogr.* **1982**, *99*, 173.

(7) (a) Klofta, T. J.; Danziger, J.; Lee, P.; Pankow, J.; Nebesny, K. W.; Armstrong, N. R. *J. Phys. Chem.* **1987**, *91*, 5646. (b) Itami, A.; Kinoshita, A.; Watanabe, K. (Konica Co.). Jpn. Kokai Tokkyo Koho, 04184448, 1992; *Chem. Abstr.* **1992**, *118*, 49228z. (c) Itami, A.; Kinoshita, A.; Watanabe, K. (Konica Co.). Jpn. Kokai Tokkyo Koho, 04184449, 1992; *Chem. Abstr.* **1992**, *118*, 49229a.

(8) (a) Yoshizawa, H.; et al. (Konica Co.). Jpn. Kokai Tokkyo Koho, 04264450, 1992; *Chem. Abstr.* **1993**, *119*, 37483m. (b) Mayo, J. D.; Duff, J. M. (Xerox Corp.). 5164493, 1992; *Chem. Abstr.* **1993**, *118*, 61527d. (c) Kinoshita, A.; et al. (Konica Co.). Jpn. Kokai Tokkyo Koho 0335064, 1991; *Chem. Abstr.* **1991**, *115*, 218800a. (d) Yamazaki, I.; et al. (Canon K. K.). Jpn. Kokai Tokkyo Koho 0384068, 1991; *Chem. Abstr.* **1991**, *115*, 194202d. (e) Yamazaki, Y. (Olympus Optical Co., Ltd.). Jpn. Kokai Tokkyo Koho 0321669, 1991; *Chem. Abstr.* **1991**, *114*, 256954r. (f) Enokida, T. (Toyo Ink Mfg. Co., Ltd.). Jpn. Kokai Tokkyo Koho 01299874, 1989; *Chem. Abstr.* **1990**, *113*, 14769w. (g) Miyamoto, E.; et al. (Mita Industrial Co., Ltd.). Eur. Pat. Appl. 314100, 1989; *Chem. Abstr.* **1989**, *111*, 164174w.

(9) (a) Oka, K.; Okada O.; Iijimaim, M. *Jpn. J. Appl. Phys.* **1993**, *32*, 3556. (b) Oka, K.; Okada, O.; Nukada, K. *Jpn. J. Appl. Phys.* **1992**, *31*, 2181.

(10) Nalwa, H. S.; Saito, T.; Kakuta A.; Iwayanagi T. *J. Phys. Chem.* **1993**, *97*, 10515.

(11) Bluhm, T.; Mayo, J.; Hamer, G.; Martin, T. *Proc. SPIE-Int. Soc. Opt. Eng.* **1992**, *1670*, 160.

(12) Hinch, G. D.; Haggquist, G. W. *Proc. SPIE-Int. Soc. Opt. Eng.* **1997**, *3144*, 16.

(13) (a) Saito, T.; Iwakabe, Y.; Kobayashi, T.; Suzuki, S.; Iwayanagi, T. *J. Phys. Chem.* **1994**, *98*, 2726. (b) Okada, O.; Klein, M. L. *J. Chem. Soc., Faraday Trans.* **1996**, *92*, 2463.

(14) Enokida, T.; Hirohashi, R.; Nakamura, T. *J. Imaging Sci.* **1990**, *34*, 234.

(15) (a) Yamashita, A.; Maruno, T.; Hayashi, T. *J. Phys. Chem.* **1994**, *98*, 12695. (b) Ghosez, Ph.; Coté, R.; Gastonguay, L.; Veilleux, G.; Denés, G.; Dodelet, J. P. *Chem. Mater.* **1993**, *5*, 1581.

(16) Gulbinas, V.; Jakubenas, R.; Pakaluis, S.; Undezenas, A. *Adv. Mater. Opt. Electron.* **1996**, *6*, 412-414.

(17) Hinch, G. D.; Voll, K. A. *Proc. SPIE-Int. Soc. Opt. Eng.* **1996**, *2850*, 181.

(18) (a) Popovich, Z. D.; Khan, M. I.; Atherton, S. J.; Hor, A.-M.; Goodman, J. L. *J. Phys. Chem. B* **1998**, *102*, 657. (b) Popovich, Z. D.; Khan, M. I.; Atherton, S. J.; Hor, A.-M.; Goodman, J. L. In *Electrical and related properties of organic solids*; Nunn, R. W., et al., Eds.; Xerox Corp.: The Netherlands, 1997; p 207.

(19) (a) Haisch, P.; Winter, G.; Hanack, M.; Lüer, L.; Egelhaaf, H.-J.; Oelkrug, D. *Adv. Mater.* **1997**, *9* (4), 316. (b) Oelkrug, D.; Lüer, L.; Egelhaaf, H.-J.; Hanack, M.; Haisch, P.; Heckmann, H.; Winter, G. *Proc. SPIE-Int. Soc. Opt. Eng.* **1997**, *3144*, 4. (c) Egelhaaf, H.-J.; Lüer, L.; Oelkrug, D.; Winter, G.; Haisch, P.; Hanack, M. *Synth. Met.* **1997**, *84*, 897.

influence of intermolecular interactions on the optical absorption spectra of single crystals (phases I and II) and evaporated films (amorphous phase, I, II, and Y) regarding molecular distortion and interplanar $\pi-\pi$ interactions, concluding that the $\pi-\pi$ interaction is quite strong in phase II, while it is relatively weak in phase I and the amorphous phase. We could confirm this behavior for the substituted analogue,^{19a} observing that only for the 2,(3)-(C₄H₉)₈PcTiO (**II**) is a successful phase transformation achieved. Additionally, we investigated the degradation provoked by the presence of oxygen of the substituted PcTiO's by varying ambient conditions and the type of solvent. We found that air-saturated solutions of these PcTiO undergo photooxidation according to first-order kinetics, whereas deoxygenated solutions are stable.^{19a} In the case of vapor-deposited films, only the crystalline phase, which we were able to show in the case of **II**, is stable with respect to photooxidation.

The aim of our ongoing research is to determine the influence on the photoconductivity of different types of substituents as well as of an enlarged π -electron system (naphthalocyanines instead of phthalocyanines) in these complexes. In the first step, we introduced electron-withdrawing substituents such as fluoroalkyl or fluoroalkoxy groups in the 1,(4)- or 2,(3)-positions of the phthalocyanine. These substituents increase both the oxidation potentials and the stability of the macrocyclic systems against photooxidation in solution.¹ In the case of the naphthalocyanine titanium(IV) oxides, we compared the tetra(*tert*-butyl)-substituted 1,(2)-naphthalocyanine (**14**) with the tetra(*tert*-butyl)-substituted 2,(3)-naphthalocyanine (**10**) with regard to their HOMO and LUMO positions and their stability and photoconductivity. Thin films of the substituted PcTiO, prepared by either vacuum deposition or spin casting, are classified into three types according to increasing intermolecular $\pi-\pi$ interactions. In this paper, we define type α , β , and γ films: type α films, characterized by absence of exciton splitting, type β films, characterized by weak exciton splitting, and type γ films, classified by a largely red-shifted B-band absorbing in the near-IR.

Synthesis

The synthetic routes to the precursors of the substituted phthalocyaninatotitanium(IV) oxides **4a-c**, **8a-c** (dinitriles **3b,c**²⁰ and isoindolines **7a-c**²¹), are shown in Scheme 1. The trifluoromethyl- and 2,2,2-trifluoroethoxy-substituted phthalocyaninatotitanium(IV) oxides (**4a-c**) are obtained from the dinitriles **3a-c**²⁰ and titanium(IV) butoxide in 1-octanol or 1-pentanol, respectively, under the conditions given in Scheme 2.

The unsubstituted 1,(2)-naphthalocyaninatotitanium(IV) oxide (**12**) has already been described in the literature.²² The highly soluble tetra(*tert*-butyl)-substituted 2,(3)-naphthalocyaninatotitanium(IV) oxide (**10**) (mixture of isomers) is synthesized, and its photoconductivity is compared with that of the PcTiO (**I**). We also synthesized **12** and the tetra(*tert*-butyl)-substituted 1,(2)-naphthalocyaninatotitanium(IV) oxide (**14**) (both mixtures of isomers as described for 1,(2)-NcFe²³). As a result of their comparable electronic properties, we did not expect effects much different from **I** for unsubstituted **12**.

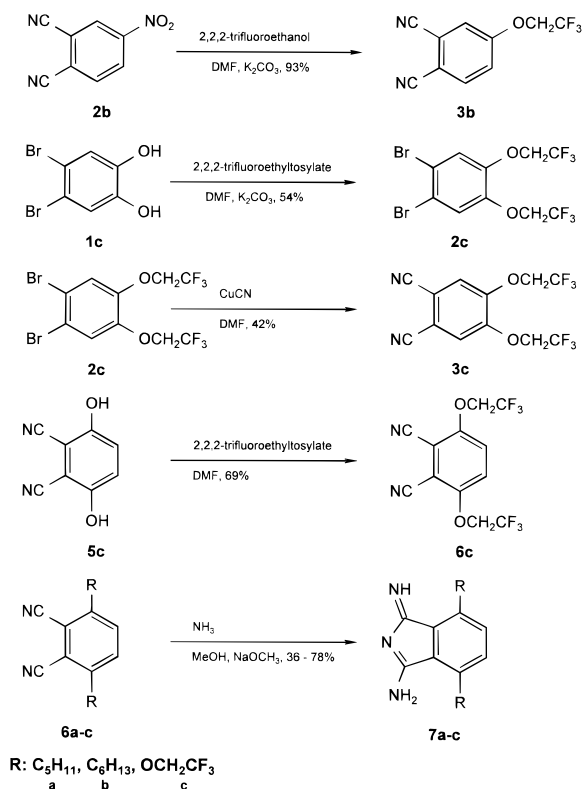
(20) Pawlowski G.; Hanack, M. *Synth. Commun.* **1981**, *11*, 351.

(21) McKeown, N. B.; Chambrier, I.; Cook, M. J. *J. Chem. Soc., Perkin Trans. 1* **1990**, 1169.

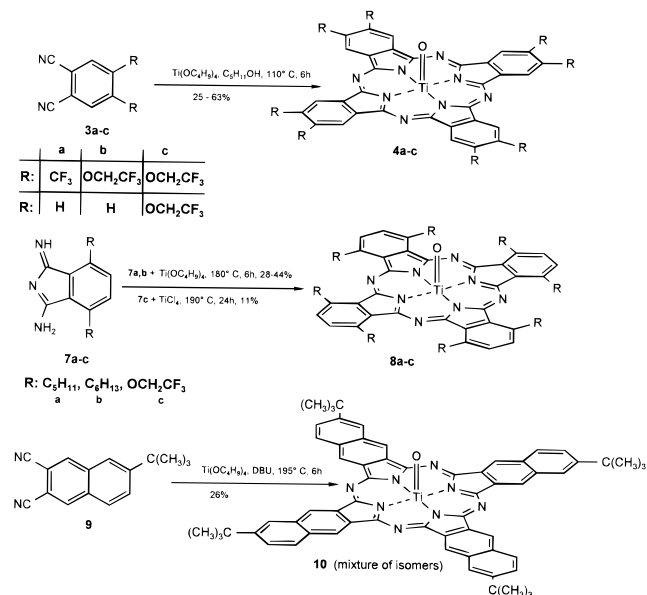
(22) (a) Tai, S.; Hayashida, S.; Hayashi, N. (Hitachi Chemical Co., Ltd.). U.S. Patent 4,842,970, **1988**. (b) Numa, T. (Nippon Kayaku Co., Ltd.). Jpn. Kokai Tokkyo Koho 63154767, 1988; *Chem. Abstr.* **1989**, *110*, 116679x.

(23) Hanack, M.; Renz, G.; Strähle, J.; Schmid, S. *J. Org. Chem.* **1991**, *56*, 3502.

Scheme 1



Scheme 2

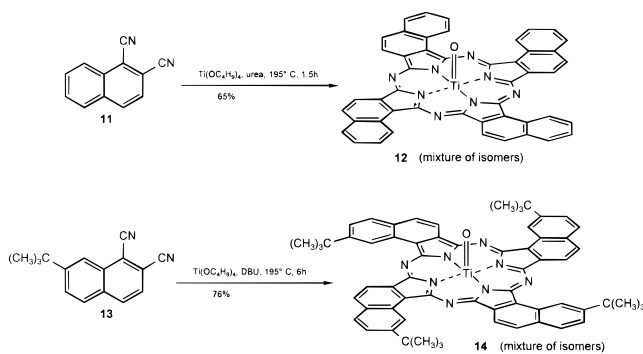


1,(4)-(C₅H₁₁)₈PcTiO (**8a**) and 1,(4)-(C₆H₁₃)₈PcTiO (**8b**) are synthesized by reacting the corresponding substituted 4,7-di-(*n*-alkyl)-1,3-diimino-1,3-dihydroisoindolines **7a,b** with titanium(IV) butoxide (Scheme 2), whereas the 2,2,2-trifluoroethoxy-substituted compound **8c** is obtained by treating the corresponding 4,7-bis(2,2,2-trifluoroethoxy)-1,3-diimino-1,3-dihydroisoindolines (**7c**) with titanium tetrachloride in 1-chloronaphthalene with addition of naphthalene to prevent the halogenation of the macrocycle.

To synthesize **10** (mixture of isomers), the dinitrile **9**²⁴ was heated with titanium(IV) butoxide and DBU in a sealed ampule

(24) Kovshev, E. I.; Puchnova, V. A.; Luk'yanets, E. A. *Zh. Org. Khim.* **1971**, *7*, 369; *J. Org. Chem. USSR* **1971**, 364.

Scheme 3



under nitrogen (Scheme 2). To prepare pure unsubstituted **12**, the corresponding 1,2-dicyanonaphthalene²⁵ (**11**) was treated with titanium(IV) butoxide and urea in *n*-octanol (Scheme 3). To avoid the formation of the metal-free naphthalocyanine, urea is a necessary additive.²⁶

In Scheme 3, the synthesis of **14** is carried out starting with 1,2-dicyano-7-*tert*-butynaphthalene (**13**), which is reacted with titanium(IV) butoxide. Compared to unsubstituted **I**,¹⁹ compounds **4b** and **8c** are soluble in acetone and THF, while **8a,b** and **10** are highly soluble in organic solvents, e.g., in THF, toluene, and dichloromethane, which allows purification by column chromatography and preparation of thin films by spin coating. The trifluoromethyl (**4a**) and the 2,2,2-trifluoroethoxy (**4b**) substituted PcTiO's are only slightly soluble in, e.g., acetone, DMF, or DMSO.

UV–Visible Absorption Spectra

Figure 2 and Table 1 present electronic absorption data in the Q-band regime measured in tetrahydrofuran solutions and in vapor-deposited or spin cast films. The extinction coefficients of the Q-band maxima have been determined to be $\epsilon = (2 \pm 0.2) \times 10^5 \text{ L mol}^{-1} \text{ cm}^{-1}$. Starting from unsubstituted **I**, the absorption maxima Q_m in solution shift upon substitution to longer wavelengths because of increasing dielectric polarizabilities of the phthalocyanine units. The strongest bathochromic shift is obtained with linear naphthalene subunits in combination with peripheral *tert*-butyl groups (**10**). When angular naphthalene subunits without peripheral substituents are introduced as in **12**, the shift reduces to very small values. This effect has been also theoretically investigated in the metal-free phthalocyanine.²⁷ The second strongest bathochromic shifts of the PcTiO are obtained with substituents in 1,(4)-positions of the benzene rings (**8a–c**) that allow conjugation with the 18 π -annulene system. The shifts decrease from alkoxy to alkyl substituents. The smallest bathochromic shifts are obtained with substituents in 2,(3)-positions of the benzene or naphthalene rings (**II**, **4a–c**, **14**) with no conjugation. The shifts reduce in the series R = alkyl (**II**), alkoxy (**III**), (trifluoroethoxy)₄ (**4b**), (trifluoroethoxy)₈ (**4c**), and trifluoromethyl (**4a**). In the last compound, the Q-band is already shifted slightly hypsochromic against the reference **I** because of the strong (–I)-effect of the CF₃ groups.

High vacuum condensation of substituted PcTiO to solid films produces new types of Q-bands, which are classified with respect to the relative shift against the Q-band maxima Q_m in solution as type α , β , and γ . This nomenclature is used for convenience

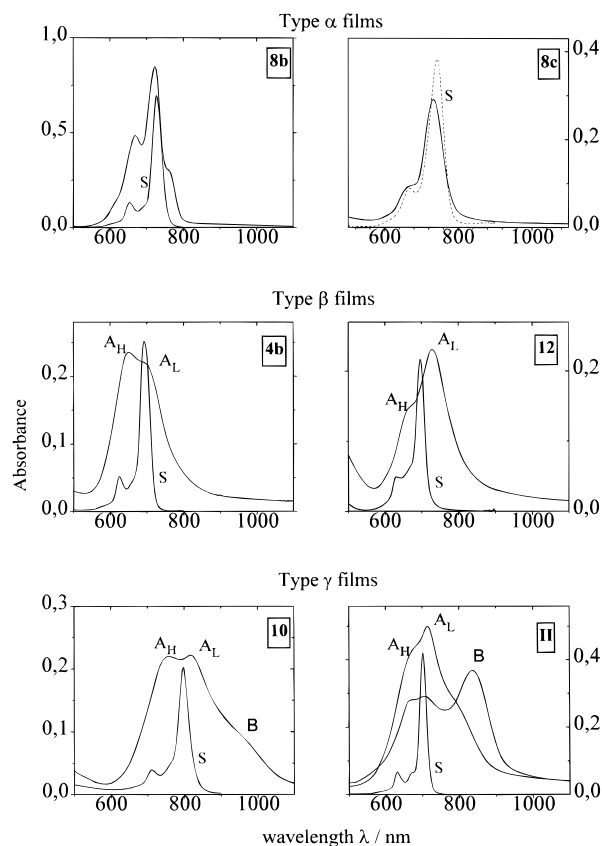


Figure 2. Electronic absorption spectra of **8b**, **8c**, **4b**, **12**, **10**, and **II** in THF solutions (labeled by “S”) and thin films. Films of **8b**, **8c**, **4b**, and **10** were prepared by spin-coating, films of **12** by vapor deposition without annealing, and films of **II** by vapor deposition at a substrate temperature of $T = 140 \text{ }^\circ\text{C}$ (curve B) and $T = 25 \text{ }^\circ\text{C}$ (curve A_H/A_L).

Table 1. Q-Band Absorption Maxima of Phthalocyaninato- and Naphthalocyaninatotitanium(IV) Oxides in THF and Thin Films ($d \approx 50 \text{ nm}$) Ordered According to Increasing Transition Energies in Solution^a

compound	THF solutions		thin films	
	Q_m (nm)	A _H (nm)	A _L (nm)	B (nm)
(<i>tert</i> -butyl) ₄ -2,(3)-NcTiO (10)	799.5	758	818	(960)
1,(4)-(CF ₃ CH ₂ O) ₈ PcTiO (8c)	741.0		732.5	
1,(4)-(C ₆ H ₁₃) ₈ PcTiO (8b)	728.5		722	
(<i>tert</i> -butyl) ₄ -1,(2)-NcTiO (14)	709.0	(650)	718	
2,(3)-(C ₄ H ₉) ₈ TiO (II) ^{19a}	700.5	666	715	836
1,(2)-NcTiO (12)	695.5	(657)	731	
2,(3)-(C ₅ H ₁₁ O)PcTiO (III) ^{19a}	695.0			
2,(3)-(CF ₃ CH ₂ O) ₄ PcTiO (4b)	691.5	641	(706)	
2,(3)-(CF ₃ CH ₂ O) ₈ PcTiO (4c)	688.5	630	720	
PcTiO (I)	686.0	(650)	713	854
2,(3)-(CF ₃) ₄ PcTiO (4a)	685.5	639	(698)	

^a Positions of shoulders are given in parentheses.

in the subsequent discussion and should not be mixed up with the depiction of polymorphs used in general for phthalocyanines. The spectra of type α films (Figure 2) are very similar to the corresponding solution spectra. The main maximum is only slightly blue-shifted by $\Delta\lambda = 5\text{--}10 \text{ nm}$ against Q_m in THF solution, and the vibrational structure of the Q-band is preserved. In some cases an additional weak peak A_L appears, red-shifted by $\Delta\lambda = 30 \text{ nm}$ against Q_m . These spectra are typical for 1,(4)-substituted PcTiO's (**8b,c**), where two of the eight substituents must be oriented perpendicularly to the phthalocyanine plane for steric reasons, thus preventing close proximity and

(25) Bradbrook E. F.; Linstead, R. P. *J. Chem. Soc.* **1936**, 1739.

(26) Yao, J.; Yonehara, H.; Pac, C. *Bull. Chem. Soc. Jpn.* **1995**, *68*, 1001.

(27) Ortú, E.; Piqueras, M. C.; Crespo, R.; Brédas, J. L. *Chem. Mater.* **1990**, *2*, 110.

Table 2. Steady-State Dark Conductivities and Photosensitivity Parameters a of Thin Films ($d = 15\text{--}70$ nm) as Well as the Ratios of Dark Conductivities in Oxygen by Dark Conductivities under Vacuum, Measured at 120 °C^a

compound	dark conductivity σ_d				irradiation wavelength, nm	film type
	σ_d , vacuum		$\sigma_{d(\text{oxygen})}/\sigma_{d(\text{vacuum})}$, $T = 120$ °C	a_{vacuum}		
	$T = 20$ °C	$T = 120$ °C				
PcTiO (I)	2×10^{-13}	7×10^{-10}	4000 ^c	1×10^{-6}	710	γ
2,(3)-(C ₆ H ₉) ₈ TiO (II)	$< 10^{-13}$	5×10^{-11}	> 350 ^c	2×10^{-8}	710	γ
(<i>tert</i> -butyl) ₄ -2,(3)-NcTiO (10)	4×10^{-11}	4×10^{-9}	1000 ^d	5×10^{-7}	850	γ
(<i>tert</i> -butyl) ₄ -1,(2)-NcTiO (14)	4×10^{-9}	1×10^{-7}	< 1	8×10^{-8}	717	β
1,(2)-NcTiO (12)	2×10^{-12}	$\approx 10^{-9}$	< 1	1.3×10^{-8}	710	β
1,(4)-(C ₆ H ₁₃) ₈ PcTiO (8b)	$< 5 \times 10^{-12}$	2×10^{-11}	b	3×10^{-9}	722	α
1,(4)-(CF ₃ CH ₂ O) ₈ PcTiO (8c)	$< 10^{-11}$	6×10^{-11}	$\approx 1/1000$	5×10^{-10}	690	α
2,(3)-(CF ₃ CH ₂ O) ₄ PcTiO (4b)	$< 10^{-11}$	6×10^{-9}	$< 1/100$	1.3×10^{-8}	640	β
2,(3)-(CF ₃) ₄ PcTiO (4a)	6×10^{-12}	6×10^{-10}	$< 1/120$	9×10^{-9}	640	β

^a Values of σ_d are given in S cm⁻¹ and values of a in S cm W⁻¹, as derived from $\sigma = \sigma_d + aL$. Irradiation intensity $L = 400 \mu\text{W cm}^{-2}$. Irradiation wavelength in nm and film type is also given. ^b No steady-state value due to rapid decomposition. ^c At 20 °C. ^d At 50 °C.

π,π -overlap of adjacent molecules in the solid state.²⁸ The distance d of neighboring phthalocyanine planes in the metal-free analogue of **8b** was determined to be $d = 8.5$ Å, more than twice the value for **I** ($d = 3.3$ Å).⁵ The spectra of type β films (Figure 2) are considerably broadened against the monomer. Two structureless absorption regions with maxima A_H and A_L are formed at the high energetic (A_H) and low energetic (A_L) sides of Q_m . The energy splittings $A_H - A_L = 0.1\text{--}0.15$ eV ($\Delta\lambda = 50\text{--}75$ nm) can be assigned within the molecular exciton model to short-range transition dipole–dipole interactions in partly ordered amorphous phases. The difference $A_H - A_L$ is very sensitive to the distance d and the intermolecular orientation of neighboring phthalocyanine planes. In the point dipole approximation, the energy splitting is proportional to d^{-3} , so that hardly any splitting is expected in type α films. In type β films, the energy splittings increase by a factor of 5–10 due to closer intermolecular distances. Either planes of adjacent molecules must be tilted, which makes both transitions A_H and A_L allowed, or the films are formed partly from sandwich aggregates (H-aggregates) and tiled roof aggregates (J-aggregates). As will be shown later, A_H is definitely more sensitive to photodecomposition than A_L , so that it is reasonable to assign the two maxima to different subphases which are simultaneously present in the films. Type β films are formed by fast deposition of unsubstituted and 2,(3)-substituted PcTiO. Fluorine-containing substituents support the intensity of A_H , while pure hydrocarbon chains support A_L . By annealing or slow deposition, the latter PcTiO can be transferred into type γ films (Figure 2 bottom), with an additional B-band in the near-infrared. From the energy difference against solution, $Q_m - B = 0.3$ eV, this band arises from dipole–dipole interactions in crystalline phases forming extended J-aggregates. In the case of unsubstituted **I**, the appearance of a B-band in the optical spectrum corresponds to the crystalline phase **II**.^{2f,9a} The presence of a similar crystal structure in type γ films of substituted PcTiO is not proven since single crystals large enough for X-ray diffraction could not be grown up to now. From EXAFS, the intermolecular Ti–Ti distance of a powder sample of **II** was determined to be $d = 4.1$ Å. To a first approximation, this value represents also the distance of neighboring phthalocyanine planes so that exciton splittings comparable to that of **I** can be expected. The transformation into type γ films can be achieved most easily with **I**, to a high degree with **II**,^{19a} and partly with **10**. However, we did not succeed until now in transforming fluorinated compounds into type γ films.

Dark Conductivity

Thin films of the PcTiO described in this paper are very weak electric conductors with dark conductivities in the range of $\sigma_d \approx 10^{-11}\text{--}10^{-9}$ S cm⁻¹ (in vacuo at $T = 120$ °C). Linear I/V characteristics have been determined up to field strengths $E = 10^4$ V/cm. As can be seen from Table 2, the dark conductivities are strongly dependent not only on temperature but also on the oxygen partial pressure of the surrounding gas phase. The oxygen dependence of conductivity was determined at $T = 120$ °C since the kinetics of interaction with oxygen is faster at elevated temperatures, and absolute conductivity values are higher than those at room temperature.

Conductivity data in vacuo at $T = 120$ °C are shown in the second column of Table 2. The dark conductivities of **8b,c** and of **II** are about 1 order of magnitude lower than that of **I**. The conductivities of **4a** and **12** are comparable to that of **I**. Finally, **10**, **14**, and **4b** are better dark conductors than **I**.

The third column of Table 2 presents the influence of oxygen exposure ($p(\text{O}_2) = 1$ bar) on the dark conductivities. The conductivities increase with **I** and its alkylated as well as linearly annulated analogues. In contrast, the conductivities decrease with fluorinated compounds **4a,b** and **8c** and with angularly annulated naphthalocyanines **12** and **14**. Figures 3 and 4 show typical examples of positive and negative influence of oxygen on the dark conductivities of phthalocyanine films. The positive influence, measured at $T = 50$ °C with a film of **10**, is rather slow, with rise times of $\tau = 10^3\text{--}10^4$ s (Figure 3). However, the kinetics of oxygen uptake can be significantly accelerated upon irradiation into the Q-bands of the samples. This can be shown by measuring dark conductivities after specified periods of irradiation during oxygen exposure (see inset of Figure 3).

An example of negative oxygen influence is presented in Figure 4 in a semilogarithmic scale. The first three half-values of σ_d are observed after exposure times of $t_{1/2} \approx 10$ s. Then the decay curve slows down, but its negative slope is still big enough to reduce σ_d after $t = 200$ s to about 2% of its value in a vacuum. The effect is reversible to a high degree since, after annealing in a vacuum, σ_d recovers to 90% of its original value.

The experimental results are correlated in the following paragraphs to the concentration N_d and mobility μ of charge carriers. Since the autoionization constant K_d of the reaction $2\text{Pc} \rightarrow \text{Pc}^+ + \text{Pc}^-$ is very low in materials formed from closed-shell neutral phthalocyanines, N_d depends strongly on the concentration of ionized donor or acceptor impurities. Dominant and unavoidable impurities under “clean” conditions are water and molecular oxygen. It is well known that oxygen favors

(28) Chambrier, I.; Cook, M. J.; Helliwell, M.; Powell, A. K. *J. Chem. Soc., Chem. Commun.* **1992**, 444.

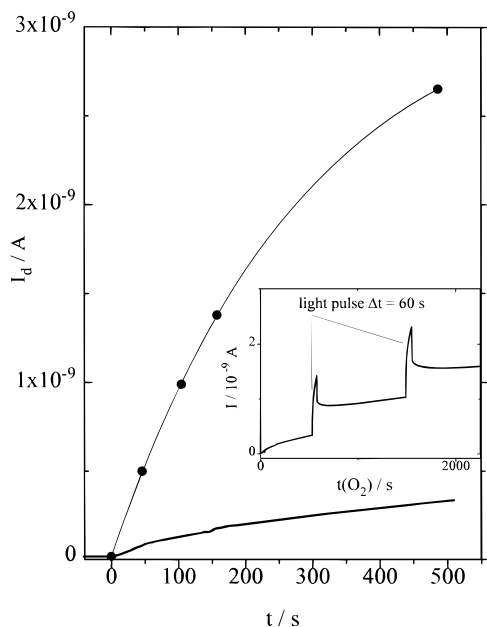


Figure 3. Dark current I_d of **10** as a function of oxygen exposure time $t(\text{O}_2)$. Lower curve, oxygen exposure in the dark; upper curve, oxygen exposure under illumination of $\lambda = 850$ nm; dark currents measured after illumination periods indicated by full points. The original measurement for curve 2 is displayed in the inset. Wavelength of light pulses $\lambda = 850$ nm. $p(\text{O}_2) = 1$ bar, $U = 50$ V, $T = 50$ °C for all measurements.

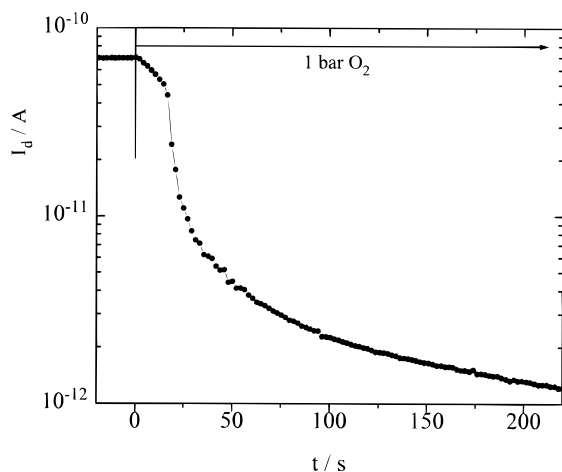


Figure 4. Dark current decay of fluorinated compound **4a** upon exposure to 1 bar oxygen at 120 °C after annealing for 16 h at $T = 150$ °C. $t = 0$ refers to start of oxygen exposure.

formation of Pc^+ according to $\text{Pc} + \text{O}_2 \rightarrow \text{Pc}^+ + \text{O}_2^-$.^{29–32} This reaction also reduces the Pc^- concentration of the autoionization equilibrium and leads, in many examples, to p-type conductance. From transient oxygen-induced dark conductivity, a CT complex PcO_2 has been postulated as precursor for charge separation by oxygen.³³ The formation tendency of this complex increases with increasing HOMO energy (i.e., decreasing ionization energy) of the phthalocyanine in the solid. Low HOMO energies, on the other hand, favor the interaction with

donors, $\text{Pc} + \text{D} \rightarrow \text{Pc}^- + \text{D}^+$, and support n-type conductance. In those cases, exposure to oxygen will reduce conductivity, because the negative majority charge carriers formed by **D** are partly compensated by the positive charge carriers formed by O_2 .

Schlettwein and Armstrong³² pointed out the importance of the HOMO position on phthalocyanine conductivity and estimated the transition from p- to n-conductance at $E_{\text{HOMO}} \approx -6.5$ eV vs vacuum. From UPS spectra, the experimental binding energy of the parent compound **I** was found by these authors at $E_{\text{HOMO}} \approx -6.3$ eV. Extension of the π -electron system as in **10** raises the HOMO level by about 0.4 eV.²⁷ The mesomeric extension in **10** is supported by additional positive inductive (+I)-effects of the alkyl substituents. These substituents alone are also able to slightly raise the HOMO level, so that finally all compounds forming type γ films (**I**, **II**, and **10**) are p-type conductors with a strong positive oxygen influence on dark conductivity (see the high $\sigma_{\text{ox}}/\sigma_{\text{vac}}$ ratios of these compounds in Table 2).

On the other hand, angularly annulated aromatic rings as in 1,(2)-naphthalocyanines **12** and **14** stabilize the HOMO level against **I** by about -0.3 eV.²⁷ Thus, the HOMO energy of **12** is located below -6.5 eV, where the transition from p- to n-type conductance is expected, and correspondingly the conductivity of **12** decreases upon oxygen exposure (see Table 2). Also, stabilization of the HOMO level by electron-withdrawing fluorine substituents as in **8c**, **4b**, and **4a** supports n-type conductance.

In addition to N_v , also the charge carrier mobilities are affected by the substituents of PcTiO . The highest values are found in unsubstituted **I** with $\mu \approx 10^{-3} \text{ cm}^2 \text{ V}^{-1} \text{ S}^{-1}$, which is still orders of magnitude lower than those in perfect organic crystals with negligible trap densities but orders of magnitude higher than those in films of conjugated polymers or oligomers, e.g., polyphenylenevinylenes or polythiophenes.²⁶ Besides the retardation effect of traps, all electronically inactive substituents slow the electron hopping rates between neighboring phthalocyanines because of larger intermolecular distances. Thus, charge carrier mobilities in type α films are expected to be orders of magnitude lower than those in type γ films, which is another reason for the measured low dark conductivities in **8b,c**.

Photoconductivity

Upon irradiation into the Q-bands of the samples, excess carriers are induced, and conductivities increase roughly linearly with light intensity L according to

$$\sigma = \sigma_d + aL \quad (1)$$

where a is the photosensitivity constant in units of S cm W^{-1} . The product aL is referred to as photoconductivity σ_p . Within the Q-band, the photosensitivity constant is independent of irradiation wavelength, indicating the vibrationally relaxed S_1 state as being a precursor for free charge carrier formation, as has been found for PcH_2 ³⁴ and PcTiO .¹⁸

Photoconductivities rise in the series type α films < type β films < type γ films (see Table 2). The dependences of σ_p on oxygen pressure are qualitatively the same as in the dark, although less pronounced. In films of alkylated compounds and **I**, σ_p rises upon oxygen exposure, whereas it decreases in fluorinated compounds and angularly annulated naphthalocyanines.

(29) Wöhrle, D.; Kreienhoop, L.; Schlettwein, D. In *Phthalocyanines, Properties and Applications*; Leznoff, C. C., Lever, A. B. P., Eds.; VCH: New York, 1996; Vol. 4, p 223.

(30) Jasunaga, H.; Kojima, K.; Johda, H.; Takeya, K. *J. Phys. Soc. Jpn.* **1974**, *37*, 1024.

(31) Musser, M. E.; Dahlberg, S. C. *Surf. Sci.* **1980**, *100*, 605.

(32) Schlettwein, D.; Armstrong, N. R. *J. Phys. Chem.* **1994**, *98*, 11771.

(33) Lüer, L.; Egelhaaf, H.-J.; Oelkrug, D. *Opt. Mater.* **1998**, *9*, 454.

(34) Noolandi, J.; Hong, K. M. *J. Chem. Phys.* **1979**, *70*, 3230.

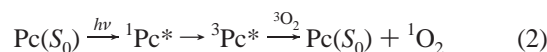
Photoinduced charge carrier formation in organic solids is known to afford impurities such as molecular O_2 acting as traps for diffusing excitons, whereupon an exciplex $(Pc^+O_2^-)^*$ is formed. Due to high intrinsic polarization, this exciplex facilitates charge separation.^{22,26,27} The existence of $(Pc^+O_2^-)^*$ in **I** and **10** was shown in transient conductivity measurements, although it has not yet been spectroscopically confirmed. We found that the formation of a ground-state CT complex $(Pc^{\delta+}O_2^{\delta-})$ during oxygen exposure is strongly accelerated by irradiation with light of Q-band absorption.²⁶ Popovich et al.¹⁸ showed the influence of water vapor on photoconductivity in PCTiO.

Crucial parameters for efficient exciplex formation are high exciton diffusion lengths and high densities of photoactive impurities. The exciton diffusion length strongly depends on the intermolecular distance d . As has already been discussed, the annulene systems in solids of 1,(4)-substituted compounds (type α films) have to be regarded as electronically isolated, d being nearly 1 nm. Thus, electronic excitation tends to be local, and exciton diffusion to an impurity is slow. Therefore, films of **8b,c** are very weak photoconductors. Type γ films of **I**, **II**, and **10**, on the other hand, display largely red-shifted B-bands in the absorption spectra, indicating long-range order and hence efficient exciton diffusion. Films of these compounds show photoconductivities sufficiently high for applications in electrophotographic devices.

The impurity density of molecular oxygen can be controlled by the O_2 partial pressure in the gas phase. Thus, photoconductivities increase in p-type conducting films upon oxygen exposure, since the density of charge separation centers forming mobile Pc^+ holes is raised. Experimentally, this behavior is observed with films of **I**, **II**, and **10**. In n-type conducting films (**4a**, **4b**, **12**, **14**, and **8c**), on the other hand, any irradiation induced Pc^+ holes produced at charge separation centers recombine with the negative majority carriers via the autoionization equilibrium. Therefore, photoconductivity decreases in n-conducting samples upon oxygen exposure.

Photochemical Stability

Stability in Solution. It is well known that π -conjugated organic molecules are sensitive to photooxidation in oxygen-containing solvents. The most important primary step is activation of 3O_2 to 1O_2 via excitation energy transfer from the excited conjugated molecule. In most phthalocyanines, the first triplet state $^3Pc^*$ lies energetically above the 1O_2 state, so the reaction



is the main route for 1O_2 formation. Thus, the amount of 1O_2 is controlled by the intersystem crossing rate of $^1Pc^*$, the lifetime of $^3Pc^*$, the oxygen concentration, and the solvent viscosity. The subsequent attack of 1O_2 on the π -electron system is also controlled by solvent viscosity and possibly by shielding substituents.

The kinetics of photodecomposition of dissolved Pc's is analyzed by the decay of Q-band absorbance as a function of irradiation time and oxygen concentration. The decay follows a first-order reaction over more than 90% of product disappearance (Figure 5). Photodecomposition of **II** yields octa(*n*-butyl)phthalimide as the clearly dominating reaction product (identified by 1H NMR, ^{13}C NMR, and MS), which supports oxidative cleavage of the annulene ring as the main photochemical reaction step. In the absence of dissolved oxygen,

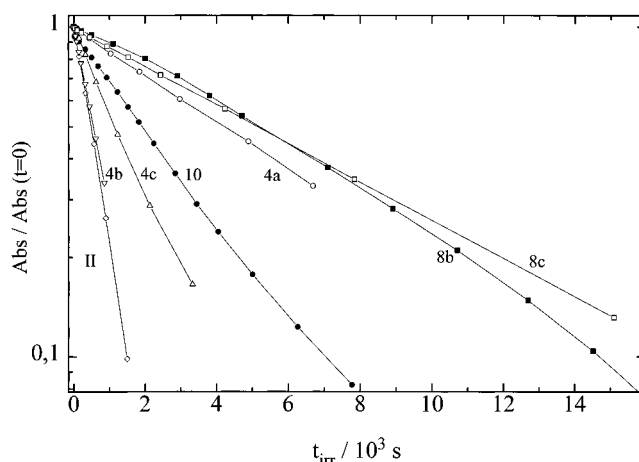


Figure 5. Photooxidation of soluble compounds in air-saturated solutions of THF under irradiation of light with $\lambda_{irr} = 670\text{--}730$ nm and intensity $L = 0.48$ mW/cm². Absorbances were measured at the Q-band maxima and normalized to $Q_{max} = 1$.

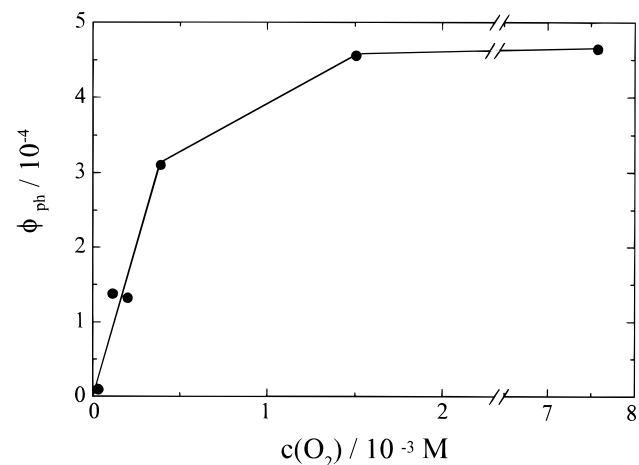


Figure 6. Dependence of the photochemical quantum yields ϕ_{ph} of **II** in toluene ($c = 5 \times 10^{-6}$ mol/L) as a function of oxygen concentration $c(O_2)$.

Table 3. Photooxidation Quantum Yields ϕ_{ph} in Air-Saturated Tetrahydrofuran (THF) Solutions and Thin Films (As-Deposited) at Room Temperature^a

compound	ϕ_{ph} (THF)	ϕ_{ph} (film)
PcTiO (I)		2×10^{-6}
(<i>tert</i> -butyl) ₄ -2,(3)-NcTiO (10)	1.6×10^{-3}	3×10^{-6}
(<i>tert</i> -butyl) ₄ -1,(2)-NcTiO (14)	3×10^{-4}	
1,(4)-Substituted		
1,(4)-(C ₆ H ₁₃) ₈ PcTiO (8b)	4.5×10^{-4}	1×10^{-3}
1,(4)-(CF ₃ CH ₂ O) ₈ PcTiO (8c)	3×10^{-4}	5×10^{-5}
2,(3)-Substituted		
2,(3)-(C ₄ H ₉) ₈ TiO (II)	7×10^{-3}	3×10^{-5}
2,(3)-(CF ₃ CH ₂ O) ₄ PcTiO (4b)	2.4×10^{-3}	3×10^{-5}
2,(3)-(CF ₃ CH ₂ O) ₈ PcTiO (4c)	1.3×10^{-3}	
2,(3)-(CF ₃) ₄ PcTiO (4a)	3.7×10^{-4}	9×10^{-6}

^a Irradiation wavelength region $\lambda = 670\text{--}730$ nm at Intensities of $L = 0.48$ mW/cm² in THF and $L = 0.65$ mW/cm² in films.

all Pc's are photochemically very stable, which can be seen from Figure 6, where the quantum yields of photodecomposition ϕ_{ph} have been plotted against the O_2 concentration. Extrapolation to oxygen-free solvents yields $\lim_{c(O_2) \rightarrow 0} \phi_{ph} = 0$.

Table 3 summarizes quantum yields of photodecomposition in air-saturated solutions. The fastest decay is found with **II**, whereas the 1,(4)-substituted PcTiO's **8b,c** are most stable against photooxidation in solution. These variations of quantum

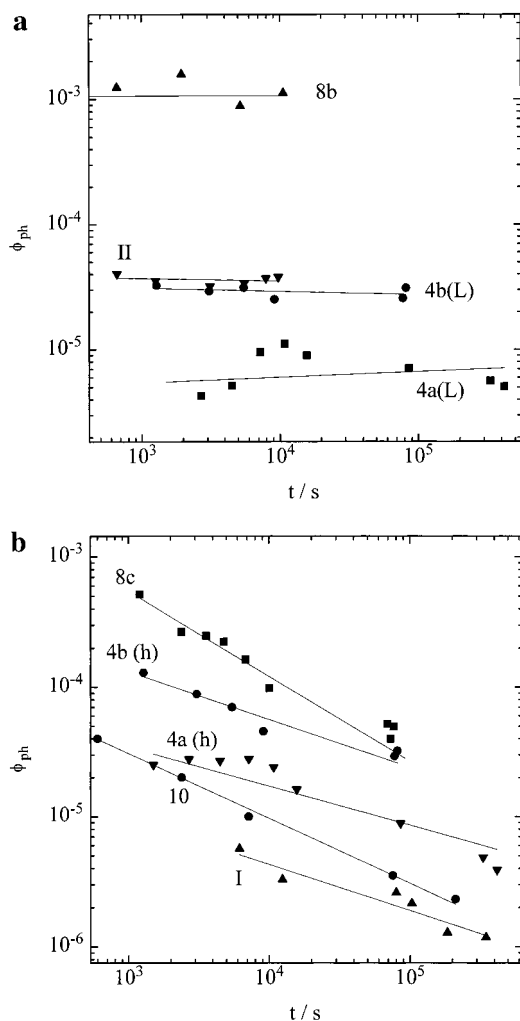


Figure 7. Dependence of photochemical quantum yield ϕ_{ph} on irradiation time. Dots: measured values of ϕ_{ph} for compounds as indicated. (h) Data from bleaching of A_{H} peak. (l) Data from bleaching of the A_{L} peak. Solid curves: fits according to $\phi_{\text{ph}} = at^{-n}$; $0 \leq n \leq 0.65$. Film thicknesses $d \approx 50$ nm, $\lambda_{\text{irr}} = 670\text{--}730$ nm with intensity $L = 0.65$ mW/cm².

yields are explained by electronic effects of the peripheral substituents. Electron-donating substituents enhance the probability of photooxidation, and electron-withdrawing substituents reduce it. With alkoxy and nitrile substituents, Sobbi et al.³⁵ described a similar effect. Substituents in 1,(4)-positions show also a stabilizing effect of about 1 order of magnitude against 2,(3)-positions; compare **4c** with **8c**, and **II** with **8b**. Fluorination and angular annulation further increases photochemical stability, as can be seen by comparing **8b** with **8c**, and **II** with **12**, respectively.

Stability of Films. Thin films of almost all compounds described in this paper are stabilized against photooxidation by about 2 orders of magnitude compared to the corresponding THF solutions (see Table 3). Compound **8b**, as the only example, is destabilized in the films. As can be seen from Figure 7a,b, the photochemical quantum yields of **8b** and **II** are independent of time (Figure 7a), whereas with **8c**, **10**, and **I**, ϕ_{ph} decreases with time according to the empirical formula

$$\phi_{\text{ph}} = bt^{-n}; \quad 0.3 \leq n \leq 0.6 \quad (3)$$

In films of the fluorinated PcTiO's **4a**, **4b**, the optical spectrum is found to change during photooxidation. In the early stages of photooxidation ($t_{\text{irr}} < 10^4$ s), A_{H} disappears more rapidly than A_{L} . As a consequence, the initial values of ϕ_{ph} for A_{H} are higher than those for A_{L} in these samples. Over the whole measuring time, ϕ_{ph} is constant for A_{L} ; it decreases with time for A_{H} .

The mechanism of photooxidation in films is not yet known. No $^1\text{O}_2$ formation could be found, and no intermediates have yet been analyzed. Since exciplex formation and photooxidation both occur in the same time domain (i.e., several days at room temperature), it is possible that the exciplex $(\text{PcO}_2)^*$ is a precursor for both charge separation and photooxidation. The latter process would then be an unavoidable parallel reaction in oxygen-induced photoconductivity. p-Type conductors with strong oxygen interaction would be more subject to photooxidation than n-type conductors. Experimentally, this is confirmed by comparing 2,(3)-substituted compounds of different HOMO energies. The fluorinated compounds **4a,b** with a stabilized HOMO level are rather stable against photooxidation, while the alkylated species **II** with an elevated HOMO level is decomposed more rapidly.

The other crucial parameter in controlling ϕ_{ph} in thin films is the diffusion coefficient of molecular oxygen D_{O_2} . In PbPc, $D_{\text{O}_2} \approx 2 \times 10^{-10}$ cm² s⁻¹ at $T = 465$ K.³⁶ A very tentative extrapolation to room temperature yields $D_{\text{O}_2} \approx 10^{-17}\text{--}10^{-19}$ cm² s⁻¹, which means that oxygen attack is restricted to the surface regions in crystalline phthalocyanines with closely packed molecular units. Photochemical quantum yields in this case are expected to be low and time-dependent, since interfacial processes such as aggregation (growth of larger crystallites at the expense of smaller ones) or passivation (surface deposition of oxidation products) lead to a decrease of free surface with time. The microcrystalline nature of **I** films is well known,^{9a} and passivation was also demonstrated with **I** by a progressive retardation of oxygen sorption kinetics over several days at $T = 100$ °C.³⁷ The time dependence of ϕ_{ph} of **I** (Figure 7b) is thus reasonably explained. In amorphous systems, the diffusion coefficient of oxygen is significantly increased due to introduction of large numbers of dislocations, yielding a quasi-homogeneous distribution of molecular oxygen in the samples. Therefore, ϕ_{ph} values in these samples are expected to be high and time-independent, as is the case with **II** (Figure 7a). The amorphous nature of **II** can be indirectly deduced from the absent contrasts in SEM micrographs and X-ray diffraction plots.³⁰ A further increase of D_{O_2} is expected if the intermolecular Pc–Pc distances are raised by spacer groups in 1,(4)-positions pointing perpendicularly to the Pc plane as in **8b**. This sterical conformation favors photooxidation by molecular oxygen dissolved in the free volume between the Pc units.

Summary

Soluble alkyl (**II**), fluoroalkyl (**4a**), and fluoroalkoxy (**4b,e**) substituted phthalocyaninato- and naphthalocyaninatotitanium-(IV) oxides **10**, **12**, and **14**, substituted in 1,(4)- or 2,(3)-positions of the aromatic rings, were synthesized and characterized with regard to their spectroscopic, photophysical, and photochemical properties to evaluate their possible use in electrophotographic devices. The solubilities in organic solvents are sufficient for spin casting of thin films. The measured photoconductivities as well as the stabilities against photooxidation were found to depend not only on the energetic HOMO positions of the film

(35) Sobbi, A. K.; Wöhrlé, D.; Schlettwein, D. *J. Chem. Soc., Perkin Trans. 2* 1993, 481.

(36) Yasunaga, H.; Kojima, K.; Yohda, H.; Takeya, K. *J. Phys. Soc. Jpn.* 1974, 37, 1024.

(37) Lüer, L.; Egelhaaf, H.-J.; Oelkrug, D. Unpublished results.

constituting molecules but also on the charge and oxygen transport properties, which are determined by the morphologies of the films. Elevation of the HOMO level by introduction of alkyl substituents in 2,3-positions or on going from phthalocyanines to 2,3-naphthalocyanines leads to high photoconductivities due to positive oxygen influence (p-type conductance) but also to enhanced photooxidation. Stabilization of the HOMO by introduction of fluorinated substituents or on going from phthalocyanines to 1,2-naphthalocyanines lowers the sensitivity against photooxidation as well as absolute photoconductivity values due to negative oxygen influence (n-type conductance).

Morphology control of the films is feasible by variation of substituents as well as film deposition parameters. Thin films of 1,4-substituted phthalocyanines with very weak intermolecular π - π interactions show low photoconductivities and are most sensitive to photooxidation. Strongest intermolecular π - π interactions are achieved by slow deposition of compounds with high electron densities in their annulene systems, i.e., alkylated 2,3-substituted phthalocyanines and 2,3-naphthalocyanines as well as the unsubstituted parent compound PcTiO. These films show the highest photoconductivities and are stabilized against photooxidation.

These results set trends for future research. Dense films with closely packed phthalocyanine units have to be formulated since, in these films, charge transport is favored over oxygen transport. Thus, high photoconductivity and photostability coincide. An elevated HOMO level of the phthalocyanines seems to be helpful in the preparation of such films, but further efforts have to be made in the investigation of the deposition parameters.

Experimental Section

Absorbances were determined using a Perkin-Elmer Lambda 2 spectrometer. The syntheses of compounds **3a**,²⁰ **7a,b**,²¹ **9**,²⁴ **11**,²⁵ **13**,²³ and 4,5-dibromocatechol³⁸ (**1c**) are described in the literature. 2,3-Dicyanohydroquinone (**5c**) is commercially available. In general, the purification of the titanium oxo complexes by column chromatography was carried out under strict exclusion of light.

2,9,16,23-Tetrakis(trifluoromethyl)phthalocyaninatotitanium(IV) Oxide (4a). A mixture of **3a** (1.5 mmol) and urea (10 mg) was heated in 1-octanol (3 mL) to 190 °C, and then titanium(IV) butoxide (174 mg, 0.51 mmol) was added while a strong stream of nitrogen was passed through the solution. The mixture was refluxed for 6 h under a slow continuous stream of nitrogen. After cooling, the mixture was poured into H₂O/MeOH/EtOH (1:1:1). The solid was centrifuged and washed with EtOH to give the crude product, which was purified by dissolving in pure acetone and centrifuging to separate the rest of the titanium(IV) oxide. This procedure was repeated, and the product was precipitated with hexane. The remainder of the dinitrile was extracted with dichloromethane in a Soxhlet apparatus. The pure product was dried under vacuum at 100 °C overnight. Yield: 102 mg (32%), dark blue powder. IR (KBr): 1622w, 1472w, 1315w, 1265m, 1171m, 1126s, 1062m, 1042m, 1008w, 906w, 841w, 746w cm⁻¹. ¹³C CP MAS NMR: δ 144.07, 132.46, 121.92. UV/vis (chlorobenzene): λ_{\max} 689.0, 621.0 nm. MS (FAB): *m/z* 847.9. Anal. Calcd for C₃₆H₁₂F₁₂N₈O₂Ti: C, 50.94; H, 1.43; N, 13.21; F, 26.88. Found: C, 50.67; H, 1.88; N, 12.80; F, 27.15.

1,2-Dicyano-4-(2,2,2-trifluoroethoxy)benzene (3b). 1,2-Dicyano-4-nitrobenzene (**2b**) (1.7 g, 10 mmol) was dissolved in anhydrous DMF (20 mL). Anhydrous potassium carbonate (30 mmol, 4.1 g) and 2,2,2-trifluoroethanol (30 mmol, 3.0 g) were then added. The mixture was stirred for about 20 h at room temperature and then finally poured into water (150 mL). The precipitate was suction filtered, washed with water and dried under vacuum. Yield: 2.1 g (93%), white solid, mp 82–83 °C. IR (KBr): 663w, 719w, 742w, 829m, 856w, 893m, 935w, 957w,

974m, 1063m, 1109m, 1159s, 1171s, 1182m, 1203w, 1254s, 1271m, 1292m, 1317m, 1408w, 1425w, 1441w, 1456w, 1491m, 1566m, 1574m, 1607m, 2235m, 2955w, 3088w, 3117w cm⁻¹. ¹H NMR (acetone-*d*₆): δ 4.95 (q, ³J_{HF} = 8.3 Hz, 2H, H-1), 7.61 (dd, ³J = 8.9 Hz, ⁴J = 2.8 Hz, 1H, H-a'), 7.80 (d, ⁴J = 2.4 Hz, 1H, H-b), 8.05 (d, ³J = 8.9 Hz, 1H, H-b'). ¹³C NMR (acetone-*d*₆): δ 66.44 (q, ²J_{CF} = 36 Hz, C-1), 109.61 (C-c'), 115.97/116.30 (C-d/d'), 118.14 (C-c), 120.95/121.27 (C-a'/b), 124.34 (q, ¹J_{CF} = 277 Hz, C-2), 136.63 (C-b'), 161.27 (C-a). ¹⁹F NMR (CD₃OD): δ -76.0 (t, ³J_{FF} = 8.6 Hz). MS (EI): *m/z* (relative intensity) 226.2 (75) [M⁺]. Anal. Calcd for C₁₀H₅F₃N₂O: C, 53.11; H, 2.23; N, 12.39. Found: C, 53.27; H, 2.59; N, 12.48.

2,9,16,23-Tetrakis(2,2,2-trifluoroethoxy)phthalocyaninatotitanium(IV) Oxide (4b). A mixture of **3b** (1.5 mmol) and titanium(IV) butoxide (3 mmol) was heated in a sealed ampule under a nitrogen atmosphere to 150 °C for 7 h. The crude product was precipitated with MeOH/H₂O/EtOH (1:1:1) and further purified by column chromatography (silica gel, hexane/acetone (1:1)). The green fraction was collected. After evaporation of the solvent under vacuum a green residue was obtained which was washed again with EtOH and dried in vacuo at 85 °C. Yield: 200 mg (55%), dark blue powder. IR (KBr): 1610s, 1487s, 1458s, 1431w, 1342s, 1288s, 1236vs, 1167vs, 1121s, 972s, 876w, 858w, 750w, 675w cm⁻¹. ¹H NMR (acetone-*d*₆): δ 9.96 (4H, H_{ar}), 7.76 (4H, H_{ar}), 8.14 (4H, H_{ar}), 4.87 (q, 8H, CF₃CH₂O). UV/vis (CH₂Cl₂): λ_{\max} 695.5, 627.0, 344.5, 280.0, 236.5 nm. MS (FD): *m/z* 968.1. Anal. Calcd for C₄₀H₂₀F₁₂N₈O₅Ti: C, 49.61; H, 2.08; N, 11.57; F, 23.54. Found: C, 50.82; H, 2.94; N, 10.26; F, 24.07.

1,2-Dibromo-4,5-bis(2,2,2-trifluoroethoxy)benzene (2c). 4,5-Dibromocatechol (**1c**) (82 mmol, 22 g), 2,2,2-trifluoroethyl tosylate (197 mmol, 50 g), and anhydrous K₂CO₃ (197 mmol, 27.2 g) were dissolved in anhydrous DMF (150 mL) and refluxed at 120 °C for 24 h under nitrogen. After cooling, the mixture was filtered, poured into water (600 mL), and extracted with CH₂Cl₂. The organic phase was washed with water and dried over MgSO₄. After evaporation of the solvent, the product was separated by column chromatography (silica gel, toluene/Et₂O (9:1), *R_f* = 0.75). Yield: 19 g (54%), waxy solid. IR (NaCl): 663m, 804w, 835w, 862m, 883m, 908w, 966s, 1057s, 1163s, 1254s, 1285s, 1360m, 1408w, 1458m, 1487s, 1589w, 2961w cm⁻¹. ¹H NMR (CDCl₃): δ 7.22 (H-2, s, 2H), 4.35 (H-1, q, 4H, ³J_{HF} = 8.0 Hz). ¹³C NMR (CDCl₃): δ 147.66 (C-a), 122.92 (C-2, ¹J_{CF} = 278 Hz), 122.13 (C-b), 118.41 (C-c), 67.88 (C-1, ²J_{CF} = 36 Hz). MS (EI): *m/z* 431.8 (M⁺). Anal. Calcd for C₁₀H₆F₆O₂Br₂: C, 27.81; H, 1.40; Br, 37.00. Found: C, 30.03; H, 1.58; Br, 35.30.

4,5-Dicyano-1,2-bis(2,2,2-trifluoroethoxy)benzene (3c). 1,2-Dibromo-4,5-bis(2,2,2-trifluoroethoxy)benzene (**2c**) (22 mmol, 9.5 g) and CuCN (66 mmol, 5.9 g) were dissolved in anhydrous DMF (100 mL) and refluxed for 8 h at 150 °C under nitrogen. After cooling, the mixture was poured into concentrated aqueous ammonia (500 mL), and air was bubbled through the solution for 24 h. The precipitate was filtered off and washed with aqueous ammonia until the filtrate was colorless and finally with water. After drying, the product was extracted in a Soxhlet apparatus with toluene for 24 h. The solvent was evaporated and the crude product was further purified by column chromatography (silica gel, toluene/ether (15:1), *R_f* = 0.3) and recrystallization from methanol. Yield: 3.0 g (42%), white crystals, mp 119 °C. IR (KBr): 663m, 891m, 972s, 1038m, 1103m, 1169s, 1217m, 1231m, 1271s, 1298s, 1362m, 1410m, 1454m, 1529s, 1582m, 1603m, 2239m, 2959w, 3074m cm⁻¹. ¹H NMR (acetone-*d*₆): δ 7.87 (H-b, s, 2H), 4.96 (H-1, q, 4H, ³J_{HF} = 8.3 Hz). ¹³C NMR (acetone-*d*₆): 151.53 (C-a), 124.33 (C-2, ¹J_{CF} = 277 Hz), 120.19 (C-b), 116.04 (C-d), 111.09 (C-c), 67.28 (C-1, ²J_{CF} = 36 Hz). MS (EI): *m/z* 324.1 (M⁺). Anal. Calcd for C₁₂H₆F₆N₂O₂: C, 44.46; H, 1.87; N, 8.64. Found: C, 44.58; H, 1.99; N, 8.55.

2,3,9,10,16,17,23,24-Octakis(2,2,2-trifluoroethoxy)phthalocyaninatotitanium(IV) Oxide (4c). A mixture of 1,2-dicyano-4,5-bis(2,2,2-trifluoroethoxy)benzene (**2c**) (1.5 mmol) and DBU (0.5 mL) was heated in 1-pentanol (3 mL) to 140 °C and then titanium(IV) butoxide (0.51 mmol, 174 mg) was added while a strong stream of nitrogen was bubbled through the solution. The mixture was refluxed for 6 h under a slow continuous stream of nitrogen. After cooling, the mixture was poured into H₂O/MeOH (1:1). The solid was centrifuged, washed with EtOH, dissolved in acetone, and suction filtered through a sintered glass

funnel (3 Å) to separate the rest of the titanium(IV) oxide. The remainder of the dinitrile was extracted with CH_2Cl_2 . The solvent was evaporated in a vacuum and the product dried under vacuum at 80 °C. Yield: 76 mg (15%), dark blue powder. IR (KBr): 2966w, 1614w, 1587w, 1489s, 1472s, 1400s, 1333m, 1263s, 1169vs, 1080s, 1053m, 1015w, 1003w, 964s, 889m, 858m, 829m, 743m, 660m cm^{-1} . ^{13}C CP MAS NMR: δ 150.9–149.2, 144.3–140.9, 131.0, 127.9, 114.3, 103.7, 70.5–65.9 (CH_2). UV/vis (acetone- d_6): λ_{max} 684.5, 619.0 nm. MS (FD): m/z 1359.0. Anal. Calcd for $\text{C}_{48}\text{H}_{24}\text{F}_{24}\text{N}_8\text{O}_9\text{Ti}$: C, 42.35; H, 1.78; N, 8.24; F, 33.52. Found: C, 39.58; H, 1.95; N, 7.62; F, 37.14.

1,2-Dicyano-3,6-bis(2,2,2-trifluoroethoxy)benzene (6c). NaOMe (62 mmol, 3.4 g) was dissolved under nitrogen in anhydrous methanol (50 mL), and 2,3-dicyanohydroquinone (**5c**) (31 mmol, 5.0 g) was added. The mixture was stirred for 2 h at room temperature. Afterward, the solvent was evaporated and the yellow residue dried under vacuum and dissolved in anhydrous DMF. After addition of 2,2,2-trifluoroethyltosylate (93 mmol, 23.6 g), the reaction mixture was refluxed for 36 h. The crude product was precipitated with water and recrystallized from EtOH. Yield: 6.9 g (69%), beige solid, mp 184 °C. IR (KBr): 644m, 689w, 720w, 758w, 839m, 860m, 970s, 1094s, 1169s, 1194s, 1259s, 1292s, 1319m, 1331m, 1425w, 1448m, 1502s, 1583w, 2232s, 2961w, 3061w, 3090w cm^{-1} . ^1H NMR (acetone- d_6): δ 4.96 (q, $^3J_{\text{HF}} = 8.4$ Hz, 4H, H-1), 7.81 (s, 2H, H-a). ^{13}C NMR (acetone- d_6): δ 67.50 (q, $^2J_{\text{CF}} = 36$ Hz, C-1), 106.63 (C-c), 113.00 (C-d), 121.33 (C-a), 124.27 (q, $^1J_{\text{CF}} = 277$ Hz, C-2), 155.23 (C-b). ^{19}F NMR (acetone- d_6): δ -75.1 (t, $^3J_{\text{FH}} = 8$ Hz). MS (EI): m/z (relative intensity) 324.0 (80) [M^+], 255.0 (10), 241.0 (100), 159.0 (90), 83.0 (100). Anal. Calcd for $\text{C}_{12}\text{H}_6\text{F}_6\text{N}_2\text{O}_2$: C, 44.46; H, 1.87; N, 8.64. Found: C, 44.51; H, 2.11; N, 8.62.

4,7-Di(pentyl)- (7a), 4,7-Di(hexyl)- (7b), and 4,7-Di(2,2,2-trifluoroethoxy)-1,3-dihydro-1,3-diiminoisoindoline (7c). Ammonia was bubbled vigorously through a solution of 3,6-di(pentyl)phthalodinitrile (**6a**) (3.7 mmol, 993 mg), 3,6-bis(hexyl)phthalodinitrile (**6b**) (6.8 mmol, 2.02 g), or 3,6-bis(2,2,2-trifluoroethoxy)phthalodinitrile (**6c**) (2.6 mmol, 900 mg) and NaOMe (45 mg) in anhydrous methanol (75 mL) for 2 h at room temperature. The stream of ammonia was then reduced to a slight current, while the solution was heated to 60 °C. The reaction was monitored by TLC (silica gel/ CH_2Cl_2) and terminated after most of the phthalodinitriles had reacted. On cooling, the diiminoisoindolines **7a–c** precipitated overnight at ca. -20 °C. The crude products were suction filtered, washed with ice cold MeOH (30 mL), and air-dried. To remove unreacted phthalodinitriles, the products were stirred in hexane, filtered, and dried in vacuo at 40 °C. They can be used for phthalocyanine formation without further purification.

7a. Yield: 377 mg (36%), reaction time 5 d, mp 135–136 °C dec. IR (KBr): 3454w, 3206m, 2957s, 2932vw, 2856m, 2723vw, 1678m, 1643w, 1620s, 1610s, 1537vs, 1441s, 1339m, 1317m, 1171vw, 1136s, 1053vw, 932vw, 822vw, 733vw, 654vw cm^{-1} . ^1H NMR (C_6D_6): δ 0.86 (t, $J = 6.6$ Hz, 6H, CH_3), 1.24–1.32 (m, 8H, γ , δ - CH_2), 1.51–1.62 (m, 4H, β - CH_2), 2.88 (broad singlet, NH), 3.05–3.14 (m, 4H, α - CH_2), 7.24 (s, 2H, H_{Ar}), 7.92, 8.53, 9.29 (broad singlets, NH). ^{13}C NMR (C_6D_6): δ 14.10 (CH_3), 22.20 (δ - CH_2), 30.19, 30.64, 31.39 (α , β , γ - CH_2), 132.42 (C-1), 135.43 (C-3), 138.60 (C-2), 158.29, 167.68, 170.46 (C-4). MS (EI): m/z 285.2 (M^+), 256.2 ($\text{M}^+ - \text{C}_2\text{H}_5$), 242.2 ($\text{M}^+ - \text{C}_3\text{H}_7$), 229.2, 184.1 ($\text{M}^+ - \text{CH}_3 - \text{C}_6\text{H}_{13}$), 170.0 ($\text{M}^+ - \text{C}_2\text{H}_5 - \text{C}_6\text{H}_{13}$), 155.0, 114.9 ($\text{M}^+ - 2\text{C}_6\text{H}_{13}$), 77.0. Anal. Calcd for $\text{C}_{18}\text{H}_{27}\text{N}_3$: 75.74; H, 9.53; N, 14.72. Found C, 76.27; H, 9.47; N, 14.45.

7b. Yield: 1.54 g (72%), reaction time 7 d, mp 116–117 °C dec. IR (KBr): 3456w, 3368vw, 3207w, 2955s, 2930vs, 2870m, 2854s, 1676m, 1620s, 1610s, 1537vs, 1441s, 1377vw, 1339m, 1315m, 1171vw, 1136s, 1059w, 922vw, 822vw, 725vw, 652vw cm^{-1} . ^1H NMR (C_6D_6): δ 0.83 (t, $J = 6.9$ Hz, 6H, CH_3), 1.20–1.31 (m, 8H, γ , δ , ϵ - CH_2), 1.49–1.60 (m, 4H, β - CH_2), 2.76 (broad singlet, NH), 2.94–3.13 (m, 4H, α - CH_2), 7.23 (s, 2H, H_{Ar}), 7.95, 8.50, 9.29 (broad singlets, NH). ^{13}C NMR (C_6D_6): δ 14.03 (CH_3), 22.17 (ϵ - CH_2), 28.63, 30.39, 30.83, 31.28 (α , β , γ , δ - CH_2), 132.29 (C-1), 134.44 (C-3), 146.01 (C-4). MS (EI): m/z 313.0 (M^+), 295.2 ($\text{M}^+ - \text{NH}_3$), 281.2 ($\text{M}^+ - \text{NH}_3 - \text{CH}_3$), 270.2 ($\text{M}^+ - \text{C}_3\text{H}_7$), 256.2 ($\text{M}^+ - \text{C}_4\text{H}_9$), 243.0 ($\text{M}^+ - \text{C}_5\text{H}_{11}$), 228.0 ($\text{M}^+ - \text{C}_6\text{H}_{13}$), 183.8 ($\text{M}^+ - \text{C}_3\text{H}_7 - \text{C}_6\text{H}_{13}$), 170.0 ($\text{M}^+ - \text{C}_4\text{H}_9 - \text{C}_6\text{H}_{13}$), 155.0 ($\text{M}^+ - \text{NH}_3 - \text{C}_4\text{H}_9 - \text{C}_6\text{H}_{13}$), 42.9 (C_3H_7^+). Formula: $\text{C}_{20}\text{H}_{31}\text{N}_3$.

7c. Yield: 0.7 g (78%), reaction time 3 d, mp 250 °C. IR (KBr): 3470m, 3339w, 3092m, 2974m, 2764w, 1657s, 1618m, 1547m, 1456s, 1427m, 1298vs, 1254vs, 1165vs, 1130s, 1086s, 972s, 881w, 858w, 833m, 798w, 710w, 652w cm^{-1} . ^1H NMR (DMSO- d_6): δ 4.96 (q, $^3J_{\text{HF}} = 8$ Hz, 4H, $-\text{CH}_2-$), 7.36 (s, 2H, H_{Ar}). ^{13}C NMR (DMSO- d_6): δ 124.0 (q, $^1J_{\text{HF}} = 278$ Hz, CF_3), 65.6 (q, $^3J_{\text{HF}} = 33$ Hz, CH_2), 167.4 (s, $\text{C}_{\text{ar}}-\text{O}$), 147.8 (NCN), 118 (C_{ar}), 120 (C_{ar}). MS (EI): m/z 342.0 (M^+), 322.1 ($\text{M}^+ - \text{F}$), 302.0 ($\text{M}^+ - 2\text{F}$), 272.1 ($\text{M}^+ - \text{CF}_3$), 243.0 ($\text{M}^+ - \text{CF}_3\text{CH}_2\text{O}$), 203.1 ($\text{M}^+ - \text{CF}_3\text{CH}_2\text{O} - 2\text{F}$), 189.1, 175.1, 161.1, 133.1, 129.1, 105.1, 83.0, 76.1, 63.1, 42.9. Formula: $\text{C}_{12}\text{H}_9\text{F}_9\text{N}_3\text{O}_2$.

1,4,8,11,15,18,22,25-Octa(pentyl)- and 1,4,8,11,18,22,25-Octa(hexyl)phthalocyaninatotitanium(IV) Oxide (8a,b). A mixture of the diiminoisoindoline **7a** or **7b** (0.61 mmol), titanium(IV) butoxide (1.5 g, 4.41 mmol), and DBU (0.5 mL) was heated in a sealed ampule under a nitrogen atmosphere to 180 °C for 6 h. The viscous oil obtained was cooled, and the phthalocyanine was isolated by column chromatography (silica gel/toluene). The first green fraction was eluted and the solvent evaporated. To achieve further purification, the product was precipitated by addition of acetonitrile, centrifuged, and dried in vacuo at 100 °C.

8a. Yield: 49 mg (28%), greenish black powder. IR (KBr): 3078vw, 3042vw, 3020vw, 2955vs, 2926vs, 2856s, 1601w, 1574vw, 1502w, 1479vw, 1466w, 1377w, 1319s, 1238vw, 1169m, 1090m, 1070m, 1001vw, 972w, 903vw, 852vw, 816vw, 760vw, 743w, 681w cm^{-1} . ^1H NMR (C_6D_6): δ 0.95 (t, $J = 7.1$ Hz, 24H, CH_3), 1.38–1.52 (m, 16H, δ - CH_2), 1.70–1.81 (m, 16H, γ - CH_2), 2.18–2.35 (m, 16H, β - CH_2), 4.59–4.85 (m, 16H, α - CH_2), 7.89 (s, 8H, H_{Ar}). ^{13}C NMR (C_6D_6): δ 14.38 (CH_3), 23.43 (δ - CH_2), 30.63, 32.14, 33.26 (α , β , γ - CH_2), 131.40 (C-1), 134.95 (C-3), 139.62 (C-2), 152.48 (C-4). UV/vis (toluene): λ_{max} 730.5, 696.0 (sh), 655.5, 359.0, 315.5 (sh) nm. MS (FD): m/z 1136.9. Anal. Calcd for $\text{C}_{72}\text{H}_{96}\text{N}_8\text{O}_2\text{Ti}$: C, 76.03; H, 8.51; N, 9.85. Found: C, 76.27; H, 8.64; N, 10.08.

8b. Yield: 84 mg (44%), greenish black powder. IR (KBr): 3076vw, 3040vw, 3017vw, 2955s, 2926vs, 2870m, 2854s, 1601vw, 1574vw, 1502w, 1466w, 1423vw, 1377vw, 1323m, 1304m, 1231vw, 1094w, 1072m, 1020vw, 972m, 906vw, 825w, 760vw, 746w, 723vw, 683vw cm^{-1} . ^1H NMR (C_6D_6): δ 0.90 (t, $J = 6.9$ Hz, 24H, CH_3), 1.28–1.49 (m, 32H, δ , ϵ - CH_2), 1.73–1.84 (m, 16H, γ - CH_2), 2.25–2.36 (m, 16H, β - CH_2), 4.58–4.86 (m, 16H, α - CH_2), 7.91 (s, 8H, H_{Ar}). ^{13}C NMR (C_6D_6): δ 14.33 (CH_3), 23.13 (ϵ - CH_2), 29.66, 30.96, 32.59, 33.35 (α , β , γ , δ - CH_2), 131.49 (C-1), 134.95 (C-3), 139.69 (C-2), 152.50 (C-4). UV/vis (toluene): λ_{max} 730.5, 696.0 (sh), 656.0, 409 (sh), 362.0, 316.0 (sh) nm. MS (FD): m/z 1249.0. Anal. Calcd for $\text{C}_{80}\text{H}_{112}\text{N}_8\text{O}_2\text{Ti}$: C, 76.89; H, 9.03; N, 8.97. Found: C, 77.96; H, 9.23; N, 9.20.

1,4,8,11,15,18,22,25-Octa(2,2,2-trifluoroethoxy)phthalocyaninatotitanium(IV) Oxide (8c). A mixture of **7c** (0.64 mmol, 200 mg) and naphthalene (0.7 mmol, 90 mg) was dissolved in anhydrous 1-chloronaphthalene (2 mL) with TiCl_4 (0.18 mmol, 0.02 mL). The mixture was heated in a sealed ampule under a nitrogen atmosphere to 190 °C for 24 h. After cooling, the crude product was centrifuged by washing with MeOH/ H_2O (1:1). The resulting viscous oil was treated with hexane to give a green powder which was purified by column chromatography (silica gel, hexane/acetone (1:1)). The green fraction was collected and evaporated under vacuum to give a green residue which was washed again with hexane and dried in vacuo at 85 °C. Yield: 45 mg (21%), greenish powder. IR (KBr): 1728, 1597, 1502, 1454, 1404, 1290, 1244, 1211, 1163, 1067, 1001, 964, 910, 833, 663 cm^{-1} . ^1H NMR (THF- d_8): δ 8.20 (s, 8H, H_{Ar}), 5.6 (q, $^3J_{\text{HF}} = 8.7$ Hz, 32H, $\text{CF}_3\text{CH}_2\text{O}-$). ^{13}C NMR (acetone- d_6): δ 152.2 ($\text{C}_{\text{ar}}-\text{O}$), 149.7 (NCN), 129.0 (q, $^1J_{\text{CF}} = 123$ Hz, CF_3), 127.6 (C_{ar}), 123.2 ($\text{C}_{\text{ar}}-\text{H}$), 70.1 (q, $^2J_{\text{CF}} = 35$ Hz, $\text{O}-\text{CH}_2-$). ^{19}F NMR (acetone- d_6): δ -74.4 (t, $^3J_{\text{HF}} = 8.6$ Hz, 24F, $\text{CF}_3-\text{CH}_2-\text{O}$). UV/vis (CH_2Cl_2): λ_{max} 745.0, 668.0 (sh), 354.5 (sh), 327.0 nm. MS (FD): m/z 1359.8. Anal. Calcd for $\text{C}_{48}\text{H}_{24}\text{F}_{24}\text{N}_8\text{O}_9\text{Ti}$: C, 42.35; H, 1.78; N, 8.24; F, 33.52. Found: C, 43.77; H 2.11; N, 7.76; F, 34.28.

3,12,21,30-Tetra(tert-butyl)-2,3-naphthalocyaninatotitanium (IV) Oxide (10). A mixture of 2,3-dicyano-6-tert-butyl-naphthalene (**9**) (0.85 mmol, 200 mg), titanium(IV) butoxide (1.7 mmol), and DBU (0.5 mL) was heated in a sealed ampule under nitrogen to 195 °C for 6 h. The oily product was precipitated with MeOH/ H_2O (1:1) and purified by column chromatography, $\text{CHCl}_3/\text{CH}_2\text{Cl}_2$ (2:1). The pure green powder

was washed with methanol and dried under vacuum at 100 °C. Yield: 87 mg (41%), dark green powder. IR (KBr): 2955m, 2905w, 1367m, 1356s, 1317m, 1271w, 1258m, 1076vs, 974m, 903m, 891w, 810w, 744w, 725w cm⁻¹. ¹H NMR (CDCl₃): δ 9.3–9.0 (m, 2H, H_{ar}), 8.6–8.0 (m, 3H) 1.9 (s, 9H, *tert*-butyl). ¹³C NMR (CDCl₃): δ 150.4, 134.5, 132.6, 130.1, 126.7, 125.2, 123.6, 123.0, 35.5 (CH₃C–), 31.7 (CH₃C–). UV/vis (THF): λ_{max} = 801.5, 714.5, 358.0, 349.5 nm. MS (FAB): *m/z* 1000.2. Anal. Calcd for C₆₄H₅₆N₈OTi: C, 76.77; H, 5.64; N, 11.20. Found: C, 76.19; H, 5.96; N, 10.82.

1,2-Naphthalocyaninatotitanium(IV) Oxide (12). A mixture of 1,2-dicyanonaphthalene (**11**) (1.1 mmol, 200 mg), titanium(IV) butoxide (100 mg), urea (10 mg), and DBU (0.5 mL) was heated in 1-octanol (2 mL) in a sealed ampule under nitrogen to 195 °C for 1.5 h. After cooling, the mixture was precipitated with H₂O/MeOH (1:1) and extracted overnight with MeOH. Yield: 177 mg (78%), dark green powder. IR (KBr): 1620w, 1584m, 1391s, 1356m, 1205m, 1155w, 1125m, 1081vs, 964s, 870w, 822s, 758s, 729s. ¹³C CP MAS NMR: δ 137.2, 137.1, 134.4, 131.4, 130.9, 130.0, 128.6 cm⁻¹. UV/vis (1-chloronaphthalene): λ_{max} 710.0, 638.0, 368.0 nm. MS (FAB): *m/z* 776.2. Anal. Calcd for C₄₈H₂₄N₈OTi: C, 74.23; H, 3.12; N, 14.43. Found: C, 75.92; H, 3.91; N, 13.64.

2,11,20,29-Tetra(*tert*-butyl)-1,2-naphthalocyaninatotitanium(IV) Oxide (14). A mixture of 1,2-dicyano-7-*tert*-butylnaphthalene (**13**) (0.85 mmol, 200 mg), titanium(IV) butoxide (1.7 mmol), and DBU

(0.5 mL) was heated in a sealed ampule under nitrogen to 195 °C for 6 h. The crude product was precipitated with MeOH/H₂O (1:1) and purified by column chromatography, CHCl₃. The pure dark blue powder was washed with methanol and dried under vacuum at 150 °C. Yield: 110 mg (76%), dark blue powder. IR (KBr): 2959s, 2907m, 2870m, 1587m, 1477s, 1460s, 1393s, 1366s, 1261m, 1196m, 1126m, 1107m, 1080m, 974m, 901w, 843m cm⁻¹. ¹³C CP MAS NMR: δ 146.7 (NCN), 129.0 (C_{ar}), 122.9 (C_{ar}), 33.0 (CH₃C). UV/vis (THF): λ_{max} 799.0, 712.5, 592.0, 358.5, 334.0, 247.0 nm. MS (FAB): *m/z* 1000.3. Anal. Calcd for C₆₄H₅₆N₈OTi: C, 76.77; H, 5.64; N, 11.20. Found: C, 75.19; H, 5.98; N, 10.62.

Acknowledgment. We are grateful to the Deutsche Forschungsgemeinschaft DFG for financial support of this research. Special thanks are expressed to the group of Prof. Dr. Bertagnolli and his co-worker Achim Weber for EXAFS measurements of **II**.

Supporting Information Available: Characterization materials for **3a,b**, **4a–c**, **6c**, **7a–c**, **8a–c**, **10**, **12**, and **14** (91 pages, print/PDF). See any current masthead page for ordering and Web access instructions.

JA981644Y